DEVELOPMENT OF TIDAL DISCHARGE AND SEDIMENT FLUX PREDICTION FUNCTIONS AT THE TIVOLI BAYS-HUDSON RIVER NATIONAL ESTUARINE RESEARCH RESERVE

A Report of the 1991 Tibor T. Polgar Fellowship Program

Christopher E. Marchesi[1]

and

Paul K. Barten[2]

1 Graduate student in Hydrology
Yale University
School of Forestry & Environmental Studies
Sage Hall
205 Prospect Street
New Haven, CT 06511

2 Assistant Professor of Water Resources
Yale University
School of Forestry & Environmental Studies
Sage Hall
205 Prospect Street
New Haven, CT 06511

ABSTRACT

A hydrologic study was conducted at the Tivoli Bays, a component of the Hudson River National Estuarine Research Reserve (HRNERR), to measure the exchange of tidal water and total suspended sediments between the Hudson River and an adjacent freshwater tidal marsh. Water flow and sediment loading were measured because of their importance as principal transport mechanisms and determinants of structure and function in aquatic ecosystems. Discharge and sediment flux measurements demonstrated a systematic pattern despite the complication of a significant tidal range generated by the lunar cycle. A set of prediction functions were constructed for both variables that account for these observed patterns. These functions can be used to estimate the total flow volume and associated sediment transport for any day of the lunar cycle. Researchers and environmental managers working in North Tivoli Bay of the HRNERR can use these functions and our methodology for environmental measurements correlated to tidal flow, such as nutrient flux and pollutant transport.

Table of Contents

Abstract..... I-3

List of Figures..... I-6

List of Tables..... I-6

Introduction..... I-7

Methods..... I-11

Results..... I-18

Discussion..... I-30

Acknowledgements..... I-36

References..... I-37

Appendix A..... I-39

List of Figures

Figure 1. Location map for Tivoli North Bay..... I-10

Figure 2A. Channel schematic showing changing water surface elevation..... I-12

Figure 2B. Channel schematic showing discharge sub-section measurements..... I-14

Figure 3. Vertical velocity profile for channel flow..... I-16

Figure 4A. Plots of discharge versus time for three selected tidal flows..... I-21

Figure 4B. Plots of sediment flux versus time for three tidal flows..... I-22

Figure 5A. Tidal flow volume histogram..... I-23

Figure 5B. Tidal sediment transport histogram..... I-24

Figure 6A. Tidal discharge prediction function for channel 1..... I-25

Figure 6B. Tidal sediment flux prediction function for channel 1..... I-26

Figure 7A. Tidal discharge prediction function for channel 2..... I-27

Figure 7B. Tidal sediment flux prediction function for channel 2..... I-28

Figure 8. Generalized discharge prediction function..... I-31

List of Tables

Table 1A. Tidal flow data for channel 1..... I-12

Table 1B. Cross-section and flow data for water level number 4..... I-14

Table 2. Discharge and sediment flux data for channel 1..... I-19

Table 3. Discharge and sediment flux data for channel 2..... I-20

Table 4. Average tidal flow velocity data..... I-34

INTRODUCTION

Estuaries are often referred to as conduits for water and associated materials on their way to larger receiving waters. Yet, in many cases, estuarine systems are sinks for much of the material flowing into them. This deposition of material has significant effects on estuarine ecosystems.

Rivers, streams, and tidal flows carry a sediment load that will vary as a function of flow dynamics and geologic conditions. This natural or baseline sediment load can be substantially increased by human activities that disturb watersheds funneling flow to the estuary. These activities include commercial and residential development, agricultural and silvicultural practices, and recreational use. This increase in sediment loading also accelerates the transport of contaminants adsorbed to sediment particles.

Lickus and Barten (1990) demonstrated the dominance of the tidal pathway on the overall water balance of Tivoli North Bay (greater than 90% of inflow). Therefore, our study focused on the tidal component as the principal source of water and suspended sediment exchanged between the Hudson River and North Bay. The primary objectives of this study included the following:

(1) Field sampling to determine flow velocity and suspended sediment concentration at North Tivoli Bay of the HRNERR, and

(2) The development of prediction functions for the exchange of tidal flow and suspended sediment transport between the Hudson River and Tivoli North Bay.

Earlier studies by Goldhammer and Findlay (1988), Lickus and Barten (1990), and Peller and Bopp (1986) estimated the tidal exchange of water and total suspended sediments between the Hudson River and the Tivoli Bays. Lickus and Barten (1990) first proposed tidal discharge versus channel water level functions. However, these earlier studies did not replicate measurements over the complete tidal range. This study was designed to develop tidal discharge and sediment flux prediction functions from data collected at a representative range of channel water levels throughout the lunar cycle.

STUDY SITE DESCRIPTION

The study site is located on the east bank of the Hudson River, north of Kingston, New York at the Tivoli Bays reserve (Figure 1). The connection between the bays and the Hudson River was altered in the 1800's following the construction of a railroad that runs from New York City to Albany. The only points of exchange for water and suspended sediments are five channels built through the railroad embankment. There are two channels on North Bay and three on South Bay. These have been numbered 1 through 5, proceeding from north to south. For a more detailed description of the Tivoli Bays see Lickus and Barten (1990). Concrete piers supporting the railroad bridges spanning the channels provided a well-defined and stable cross-section for flow velocity measurements. The channel bottoms are lined with loosely laid stone blocks, which further stabilize the channels. The horizontal upper surfaces of the bridge abutments also provided a fixed reference point for water level measurements.

The lunar cycle has a marked influence upon the tidal flow exchanged through the channels despite their location 100 miles (161 Km) upstream of the Battery in New York City. Water levels fluctuated by up to 6 feet (1.8 meters) from flood to ebb tides. The water surface elevation at low tide varied little throughout the lunar cycle. However, the water surface elevation at high tide varied by as much as 3 feet (0.9 meters).

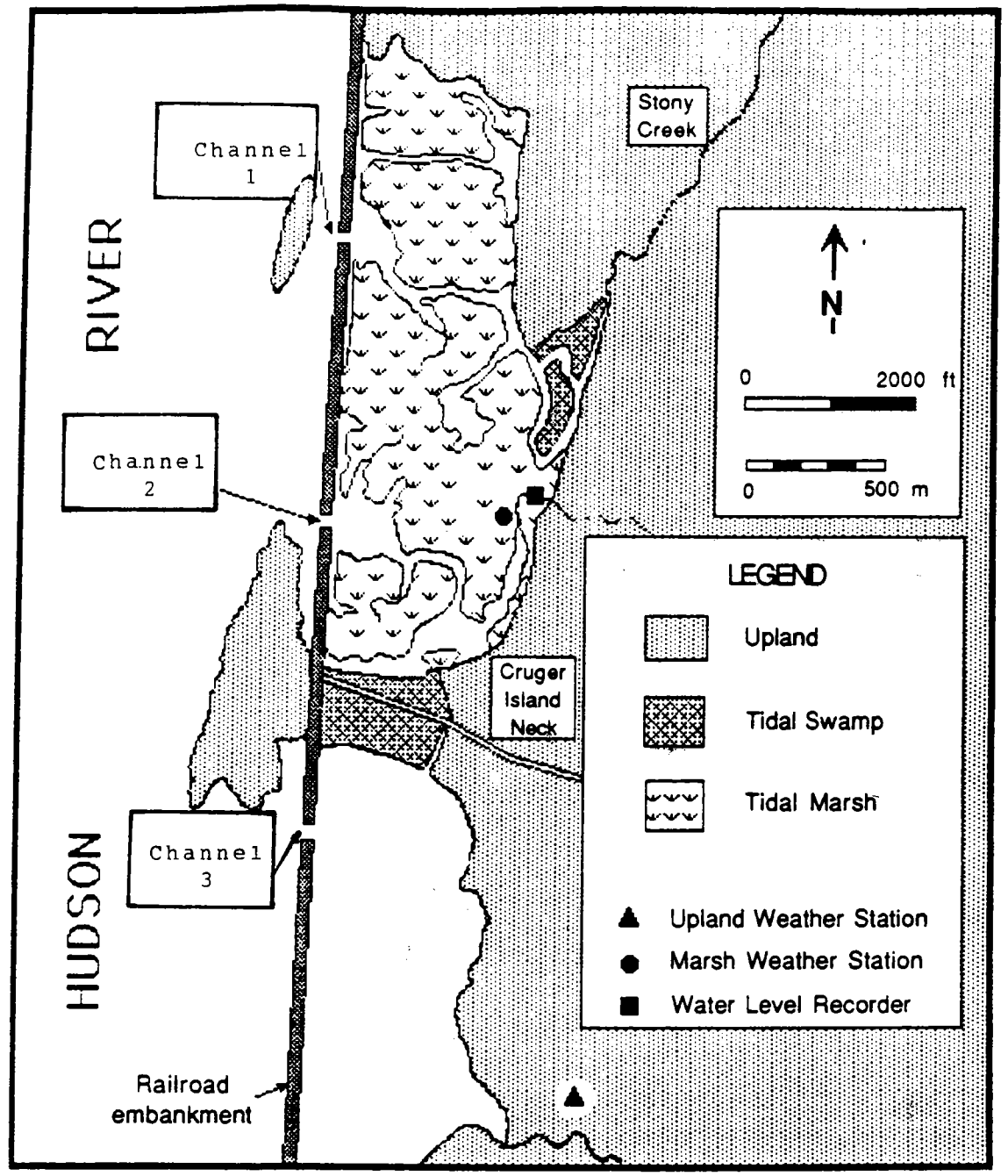

Figure 1: Location map of North Tivoli Bay (Lickus and Barten, 1990)

METHODS

There were two components to the field sampling conducted during June, July, and August, 1991, (1) the collection of data required to calculate the total volume of flow exchanged between the Hudson River and Tivoli North Bay via bridge channels 1 and 2 (Figure 1), and (2) the collection of suspended sediment data for a range of tidal discharges.

Tidal Flow Measurements

The collection of tidal flow data and the subsequent calculation of tidal discharge includes a number of steps, which are best explained with an illustration. Figure 2A is a scale drawing of bridge channel 1. The first step in the measurement of discharge (ft^3/sec) was to locate a cross-section of uniform flow (Dunne and Leopold, 1978). Cross-sections were located at either end of the bridge abutments where pilings did not generate turbulence or other disturbances to the flow path.

The fundamental equation for the calculation of discharge is:

$$Q = A * V \quad (1)$$

where Q is discharge (ft^3/sec), V is flow velocity (ft/sec), and A is the cross-sectional area of the channel (ft^2). Figure 2A shows the increase of the water surface

Figure 2A Channel schematic showing changing water surface elevation. Companion table (1A) includes the data from which figure 2A was developed.

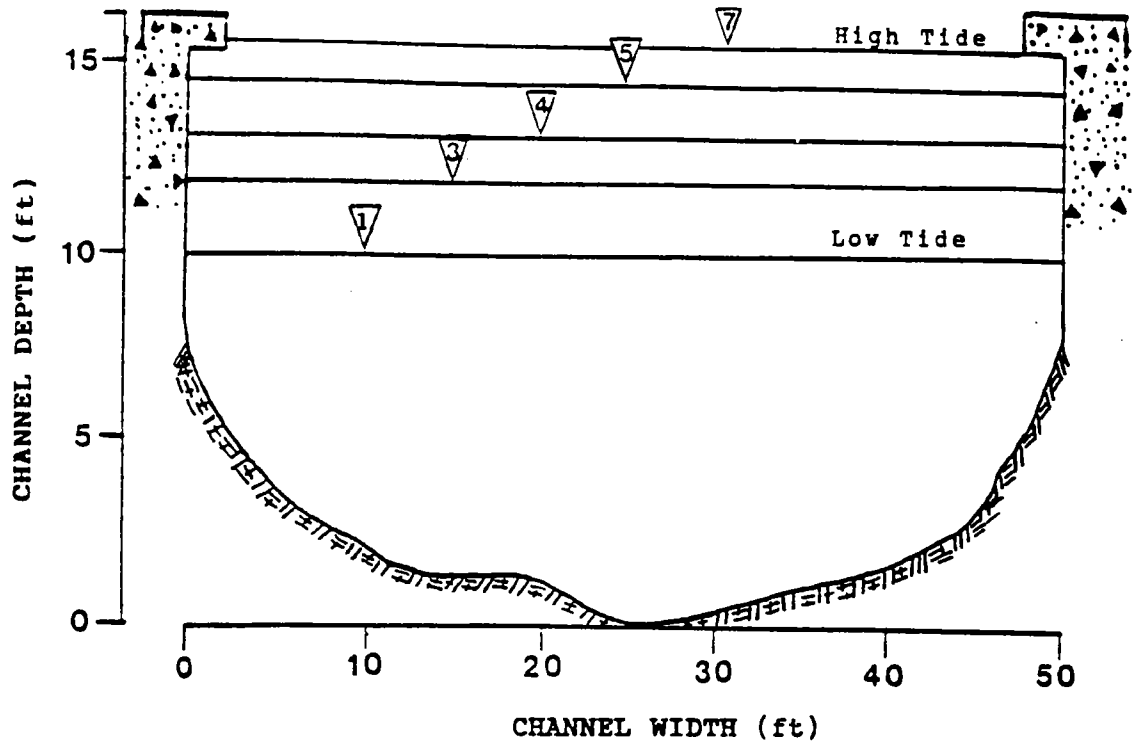

Table 1A Tidal flow data for channel 1, HRNERR July 16, 1991.

Water surface	Time (hrs)	Water Level* (ft)	Area (ft^2)	V** (ft/sec)	Discharge (ft^3/sec)
1 (L-tide)	0	6.5	362	0	0
.	.	.	.	.	.
.	.	.	.	.	.
3	1.42	5.1	452	0.81	365
4	2.32	4.0	528	1.04	550
5	3.13	3.2	587	1.06	620
.	.	.	.	.	.
.	.	.	.	.	.
n (H-tide)	6.00	2.0	612	0	0

* Water level is measured from top of bridge abutment down to water surface.
** Mean velocity = Discharge/Area

elevation during the progression of channel inflow from low tide to high tide (flood tide). Ebb tides are the outflow of water from within the bay to the Hudson River during the progression from high tide to low tide. The total volume of flow for either a flood or ebb tide is determined by integrating the area under a plot of discharge versus time. Such plots are constructed from instantaneous discharge values corresponding to the positive or negative progression of the water surface elevation during the approximate six hour tidal flow period. Table 1A includes the data from which Figure 2A was developed - a flood tide that was measured at channel 1 on July 16, 1991. The last column in Table 1A lists discharge values for selected water surface elevations (▽n) during the flood tide. The mean-section method was used to calculate discharge at each of these water levels (Butler, 1957).

Figure 2B is a channel schematic showing sub-section measurements to determine total discharge using the mean-section method for water elevation 4 during a flood tide at channel 1, July 16, 1991. Table 1B is the companion table for Figure 2B; it contains the cross-section and flow velocity data for water surface elevation 4. The mean-section method divides the cross-sectional area of the channel into a series of trapezoidal sub-areas, each flowing at uniform velocity equal to the mean of the velocities at the two bordering depth-observation positions (Butler, 1957). The mean velocity was calculated using the equation

Figure 2B Channel schematic showing sub-section measurements to determine total discharge

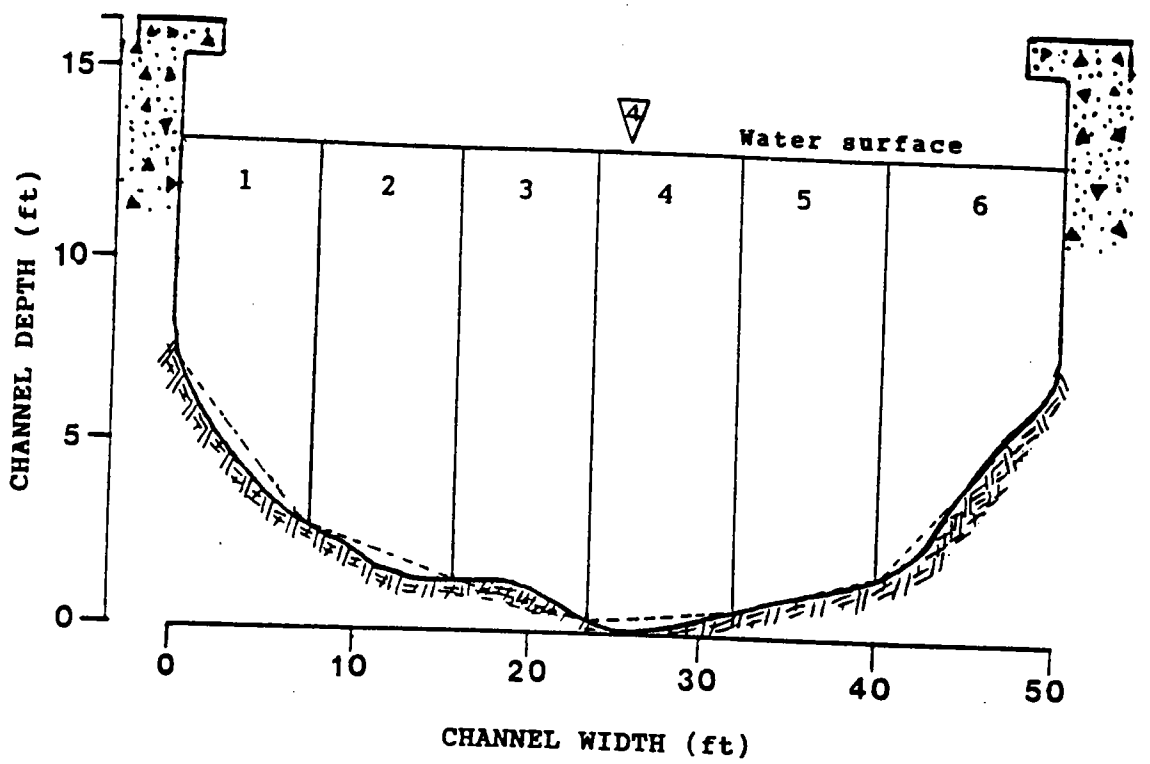

Table 1B Cross-section and flow velocity data for run number 4 (see Table 1A), Channel 1, HRNERR, July 16, 1991.

Distance From Abutment (ft)	Flow Depth (ft)	Sub-Section Number	Area A (ft^2)	Velocity (ft/sec)	Discharge Q (ft^3/sec)
0	5.0				
8	11.0	1	64	0.17	10.9
16	12.0	2	92	0.68	62.7
24	13.0	3	100	1.13	113.0
32	12.5	4	102	1.65	168.3
40	10.5	5	92	1.58	145.4
50	5.0	6	78	0.63	50.0

i=Individual Measurements $\sum A_i = 528\ ft^2$ $\sum Q_i = 550\ ft^3/s$

$(V_L+V_R)/2$, where V_L is the measured flow velocity at the left vertical, and V_R is the flow velocity at the right vertical for each trapezoid show in Figure 2B. The area of each trapezoid was determined from data listed in Table 1B. Sub-unit discharge values were calculated and summed across the channel to obtain total discharge using equation 2.

$$Q = \sum_{i=1}^{n} A_i * V_i \qquad (2)$$

Total discharge is equal to the sum of the products of individual sub-areas and average velocities for n number of subdivisions. Figure 2B is simplified by showing only six subareal divisions, but our field measurements included a minimum of twelve.

Flow velocity and channel depth measurements were taken from a boat tethered to a taut line spanning the channel bridge abutments. The line served to stabilize and guide the boat as measurements were taken at regular intervals of width. Flow velocity was measured at six-tenths depth (below the water surface) using a Qualimetrics^{TM} 6660 current meter. Flow velocity at six-tenths depth has been empirically determined to represent the position in the water column of mean velocity (Linsley et al., 1975). Figure 3 is a vertical velocity profile showing this position of average velocity.

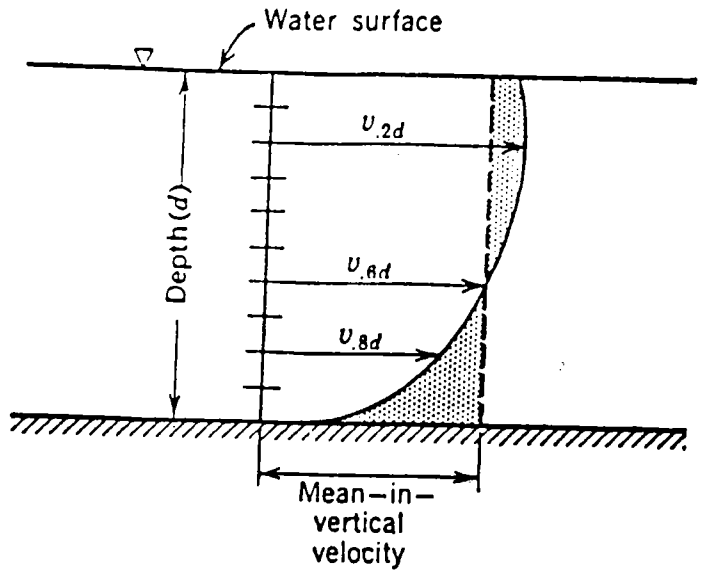

Figure 3: Vertical velocity profile for channel flow. Mean vertical flow velocity occurs at six-tenths depth (Butler, 1957).

Total Suspended Sediments

Suspended sediment samples were collected over a full range of water levels for both flood and ebb tides. These values were then used to calculate total sediment transport for a complete tidal cycle.

The suspended sediment sampling method used was modelled after a United States Geological Survey system (Guy and Norman, 1970). This is a depth integrating technique where the sampler is lowered to the bottom of the channel and immediately pulled upward at a steady velocity through the water column. The resulting sample is representative of the vertical variation of the suspended sediment load within the water column. Suspended sediment samples, taken in duplicates, were paired with discharge values for each water surface elevation.

Laboratory Analyses

Water samples were analyzed for total suspended sediments at Yale University's Greeley Laboratory. The standardized USGS filtration method was used to determine the suspended sediment concentration (Guy, 1969). The total volume of each sample was recorded followed by drawing them through a filter apparatus consisting of a Gooch Crucible and filter paper sized to trap all organic and inorganic (sand, silt, and clay) material. Glass fiber filter disks (Corning, #934-AH) were used, which are designed to remain unaffected by the filtration process and subsequent desiccation. Following filtration, the filter papers were dried in a laboratory oven at 110^{o}C for at least one hour. This removed any residual moisture that would effect the final weight. The final step was a calculation of concentration by dividing the weight of the filter residue by the sample volume (mg/l or ppm).

RESULTS

A total of eleven tidal flows were measured at channels 1 and 2 of Tivoli North Bay. Discharge and sediment flux data for each tidal flow are summarized in Tables 2 and 3. Figure 4A is a plot of discharge versus time data for three selected flood tides taken from Table 2. Figure 4B is a plot of sediment flux versus time data for the same three flood tides. Both plots are necessary for calculating the total flow volume and mass of sediment transported for each tidal flow. However, these plots will not yield generic prediction functions for discharge and sediment flux because time is constant while both discharge and sediment flux are highly variable throughout the lunar cycle. Figures 5A and 5B are histograms that illustrate the variability in total flow volume and mass of transported sediment for the eleven tidal flows measured. Therefore, our objective was to derive a set of prediction functions capable of representing this variability.

Figures 6A and 6B show discharge versus flow depth and sediment flux versus flow depth for channel 1. Figures 7A and 7B show discharge versus flow depth and sediment flux versus flow depth for channel 2. Flow depth (stage) is the linear measurement taken between the water surface and the deepest point of the channel cross-section. These predictions functions show the direct relationship between channel stage and discharge and sediment flux.

Table 2 Discharge and sediment flux data for three flood and three ebb tides measured at channel 1, Tivoli North Bay, HRNERR, 1991. The last two columns list the total flow volume and mass of sediment transported for each tidal flow.

Tide	Time (hr)	Flow Depth (ft)	Discharge (ft^3/sec)	Sediment (g/sec)	Total Flow Volume (ft^3*10^6)	Total Sediment (Kg)
Flood Tide 1						
Low	0	9.3	0	0		
	.25	9.5	11.5	6.9		
	1.08	10.2	125.7	155.5		
	1.85	10.6	341.9	567.1		
	2.62	11.6	379.4	116.5		
	3.52	12.6	507.0	209.7		
	4.47	13.0	672.9	230.8		
	5.38	13.8	626.5	212.2		
High	6.05	14.0	0	0	8.2	4500
Flood Tide 2						
Low	0	9.3	0	0		
	.88	10.0	253.3	372.3		
	1.42	10.7	365.1	92.7		
	2.32	11.9	576.6	213.7		
	3.13	13.0	569.4	216.1		
	4.25	13.5	856.2	279.6		
High	5.63	13.8	0	0	9.2	3850
Flood Tide 3						
Low	0	9.4	0	0		
	1.02	9.6	103.0	50.0		
	1.88	11.0	342.0	121.0		
	2.87	11.2	473.8	92.6		
	3.75	11.6	473.9	77.6		
	4.97	12.0	290.9	58.0		
High	5.55	12.2	0	0	5.8	1350
Ebb Tide 1						
High	0	12.1	0	0		
	.47	12.0	254.7	54.8		
	1.65	11.7	551.7	118.9		
	2.65	11.0	358.2	113.1		
	3.72	10.5	332.3	69.4		
	4.65	10.0	208.6	61.9		
	5.85	9.4	133.3	45.0		
Low	6.60	9.3	0	0	6.7	1700
Ebb Tide 2						
High	0	11.7	0	0		
	.40	11.6	163.1	29.8		
	1.23	11.5	303.2	48.8		
	2.25	10.9	314.0	74.2		
	3.83	10.5	226.3	56.0		
	4.40	10.0	185.0	56.3		
	5.23	9.3	119.1	37.6		
Low	5.70	8.9	0	0	4.4	1000
Ebb Tide 3						
High	0	12.8	0	0		
	.88	12.5	818.8	327.0		
	1.63	12.2	984.4	595.5		
	2.53	11.5	634.5	331.9		
	3.52	10.8	385.6	192.6		
	4.55	10.2	210.0	91.4		
	5.32	9.8	143.8	53.3		
Low	6.45	8.9	0	0	10.1	5000

Table 3 Discharge and sediment flux data for three flood and two ebb tides measured at channel 2, Tivoli North Bay, HRNERR, 1991. The last two columns list the total flow volume and mass of sediment transported for each tidal flow.

Tide	Time	Flow Depth	Discharge	Sediment	Total Flow Volume	Total Sediment
	(hr)	(ft)	(ft^3/sec)	(g/sec)	(ft^3*10^6)	(Kg)
Flood Tide 1						
Low	0	9.10	0	0		
	.18	9.20	41.7	22.3		
	1.75	10.3	172.4	67.1		
	2.30	10.5	279.1	84.6		
	3.32	11.4	424.3	90.5		
	4.05	11.8	453.8	99.7		
	4.90	12.3	336.3	69.1		
High	5.33	12.5	0	0	5.0	1300
Flood Tide 2						
Low	0	9.0	0	0		
	.43	9.2	42.3	18.5		
	1.08	9.8	149.3	42.0		
	2.05	10.8	421.9	101.9		
	3.17	11.8	674.3	243.9		
	4.28	12.1	814.4	220.7		
	5.00	12.9	494.7	99.3		
High	5.67	13.0	0	0	9.3	2600
Flood Tide 3						
Low	0	9.2	0	0		
	.45	9.4	42.4	24.0		
	1.20	10.2	175.1	-		
	1.95	10.8	331.5	92.3		
	2.92	11.2	609.0	148.7		
	3.92	12.1	845.2	186.0		
	4.97	12.5	687.5	136.5		
High	5.70	13.1	0	0	9.1	1800
Ebb Tide 1						
High	0	11.9	0	0		
	.52	11.8	170.5	53.2		
	1.40	11.2	410.8	158.6		
	2.40	10.8	317.1	127.7		
	3.62	9.8	134.7	41.3		
	4.73	8.9	104.3	29.4		
Low	6.17	8.3	0	0	4.1	1400
Ebb Tide 2						
High	0	10.6	0	0		
	.35	10.5	58.3	12.6		
	1.33	10.3	-	-		
	2.27	10.4	116.0	24.0		
	3.07	10.2	166.6	43.9		
	4.05	9.8	160.6	50.5		
	4.83	9.2	76.6	23.3		
Low	5.92	8.7	0	0	1.9	500

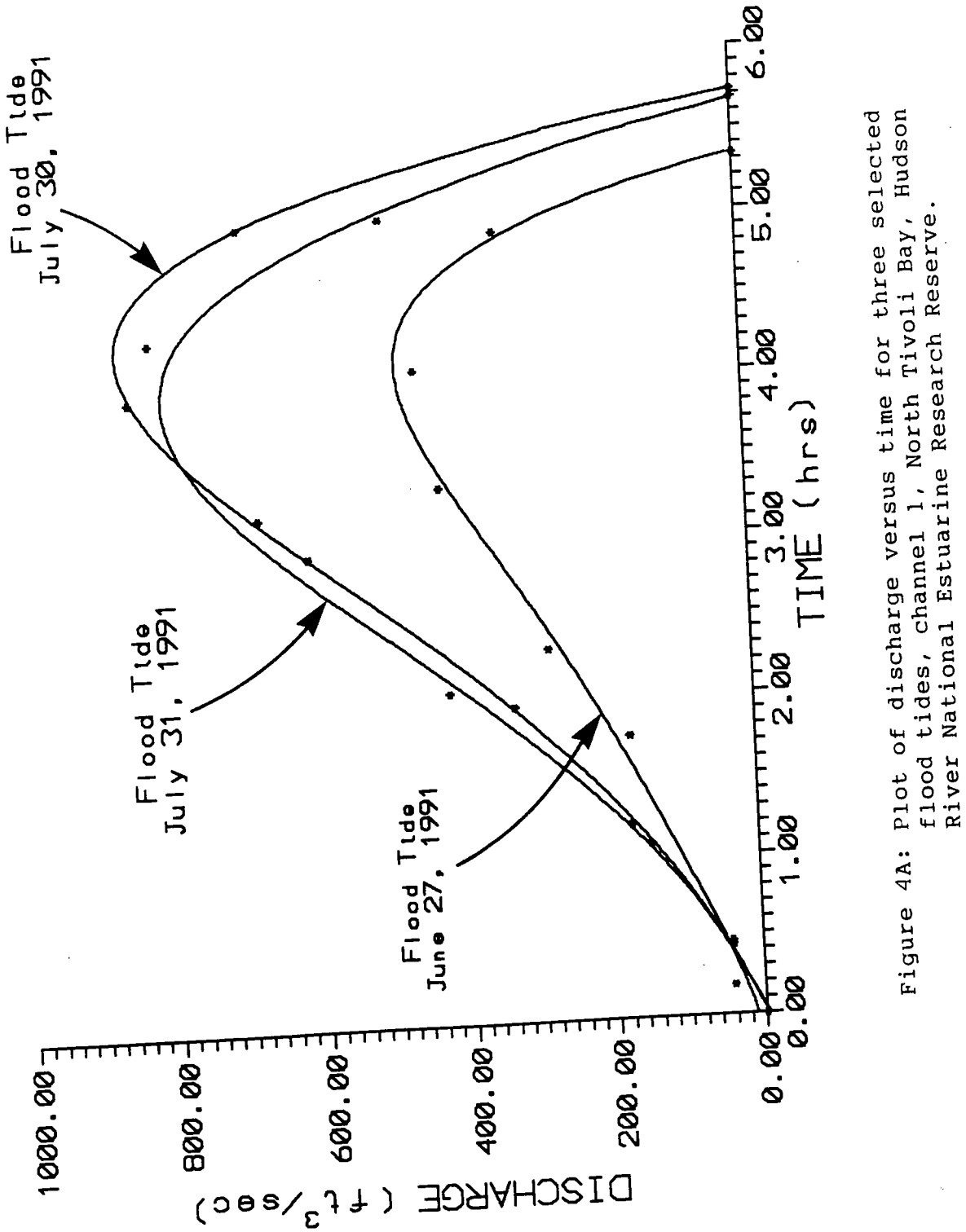

Figure 4A: Plot of discharge versus time for three selected flood tides, channel 1, North Tivoli Bay, Hudson River National Estuarine Research Reserve.

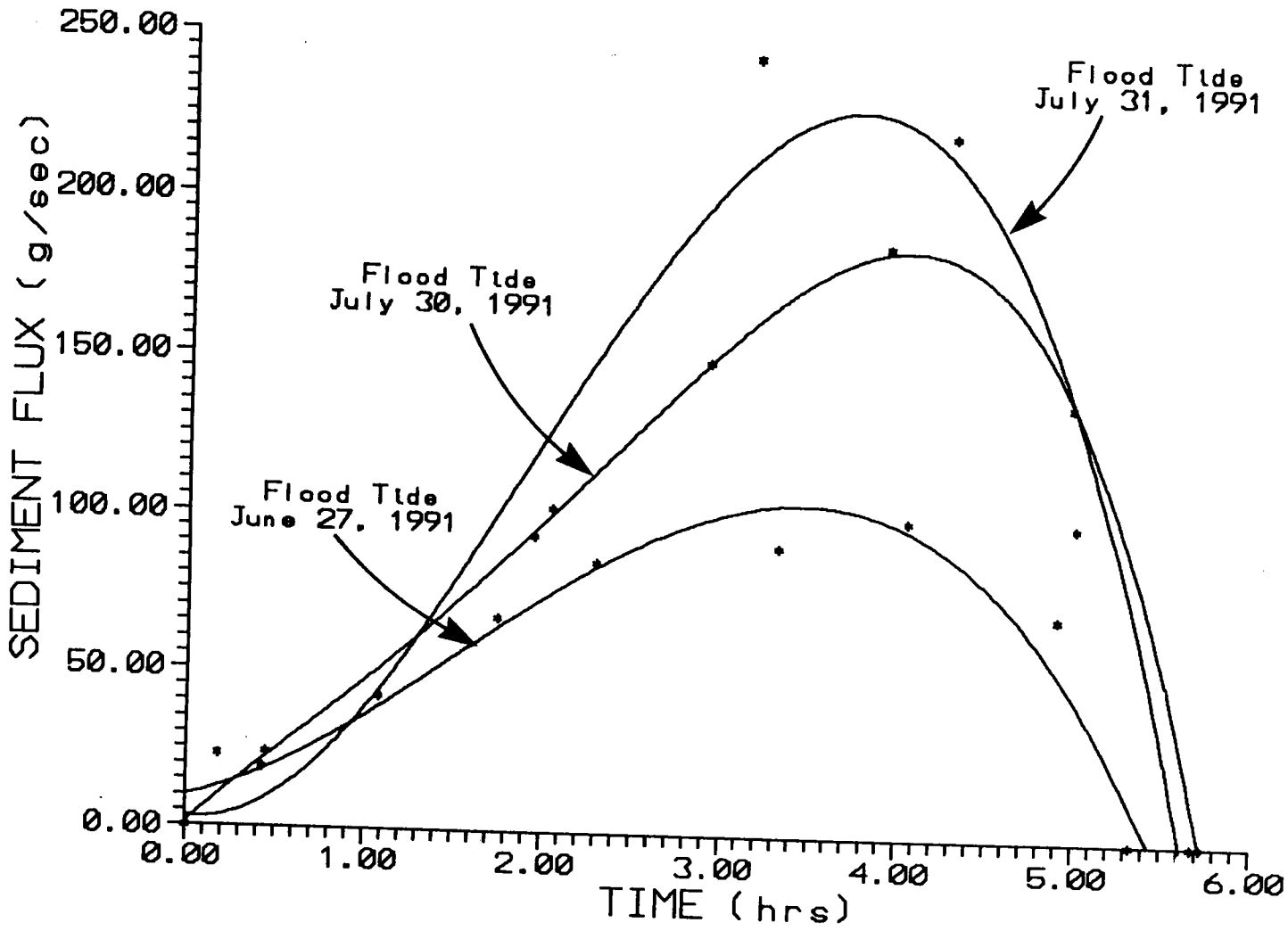

Figure 4B: Plot of sediment flux versus time for three flood tides corresponding to the plots of discharge in Figure 5A, channel 1, North Tivoli Bay, Hudson River National Estuarine Research Reserve.

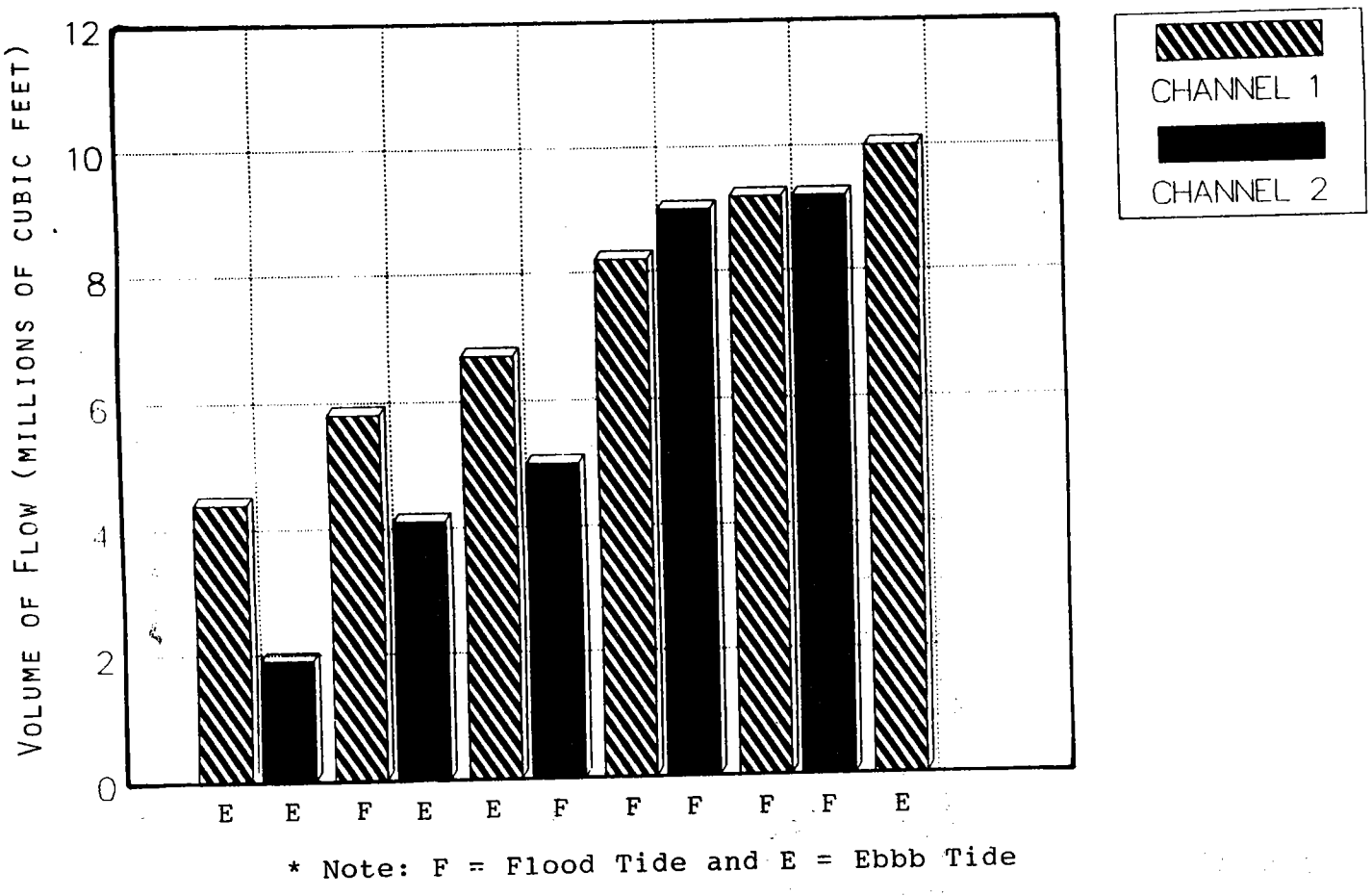

Figure 5A: Total tidal flow volume for eleven flood and ebb tides measured at channels 1 and 2, Tivoli North Bay, HRNERR.

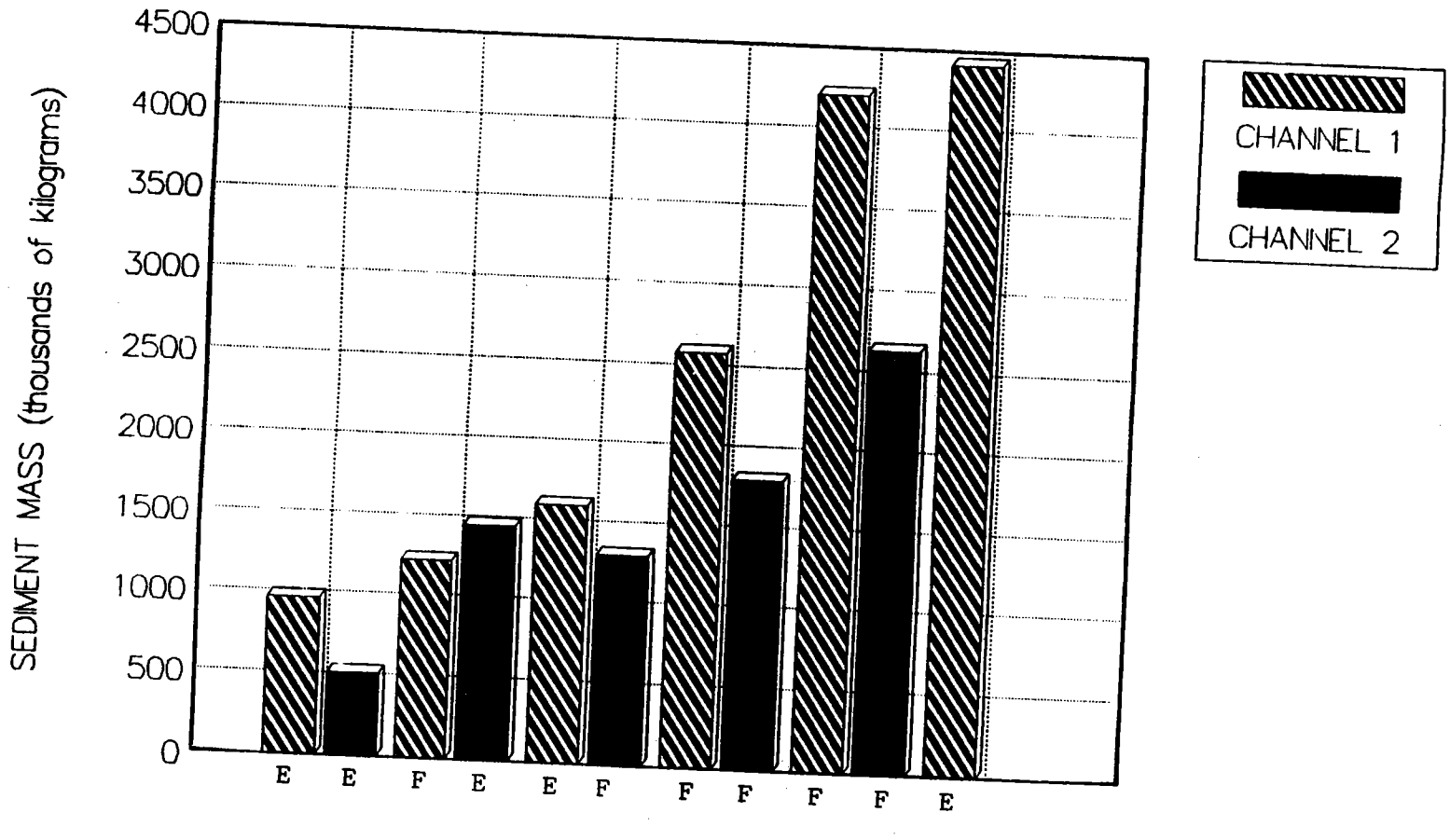

* Note: F = Flood Tide and E = Ebb Tide

Figure 5B: Total mass of sediment for the eleven tidal flows shown in Figure 5A.

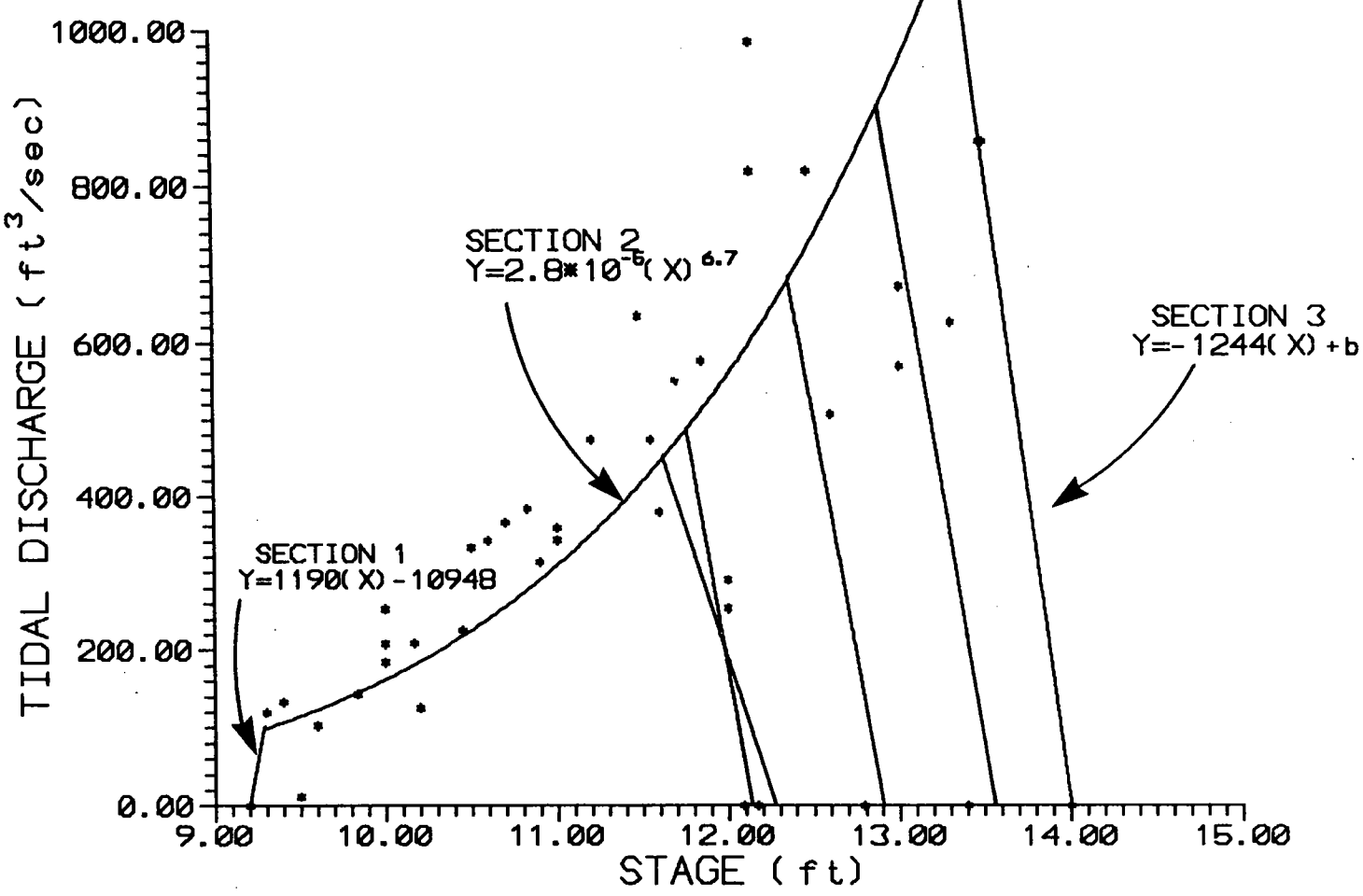

Figure 6A: Tidal discharge prediction function for channel 1, Tivoli North Bay, Hudson River National Estuarine Research Reserve.

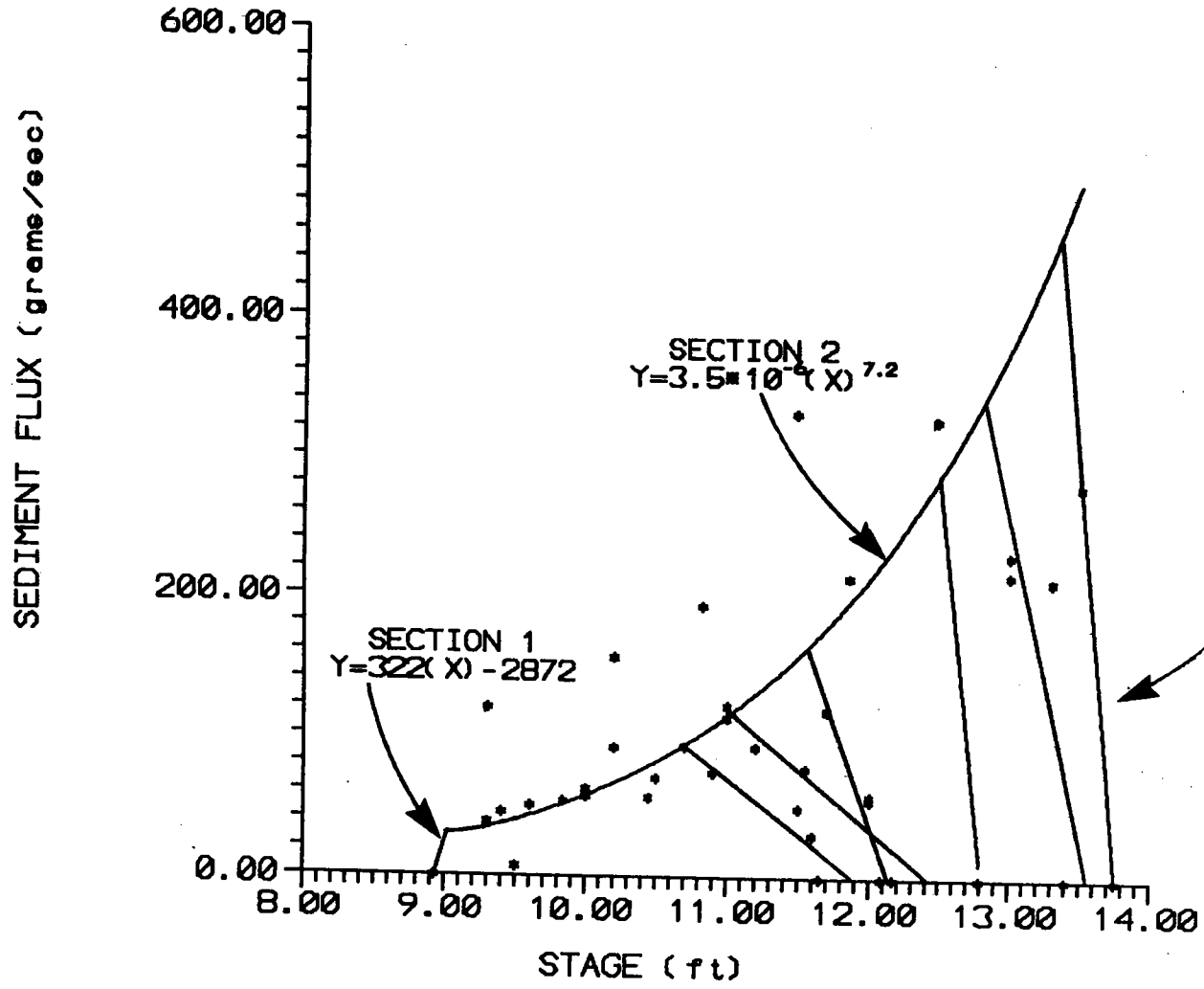

Figure 6B: Tidal sediment flux prediction function for channel, Tivoli North Bay, Hudson River National Estuarine Research Reserve.

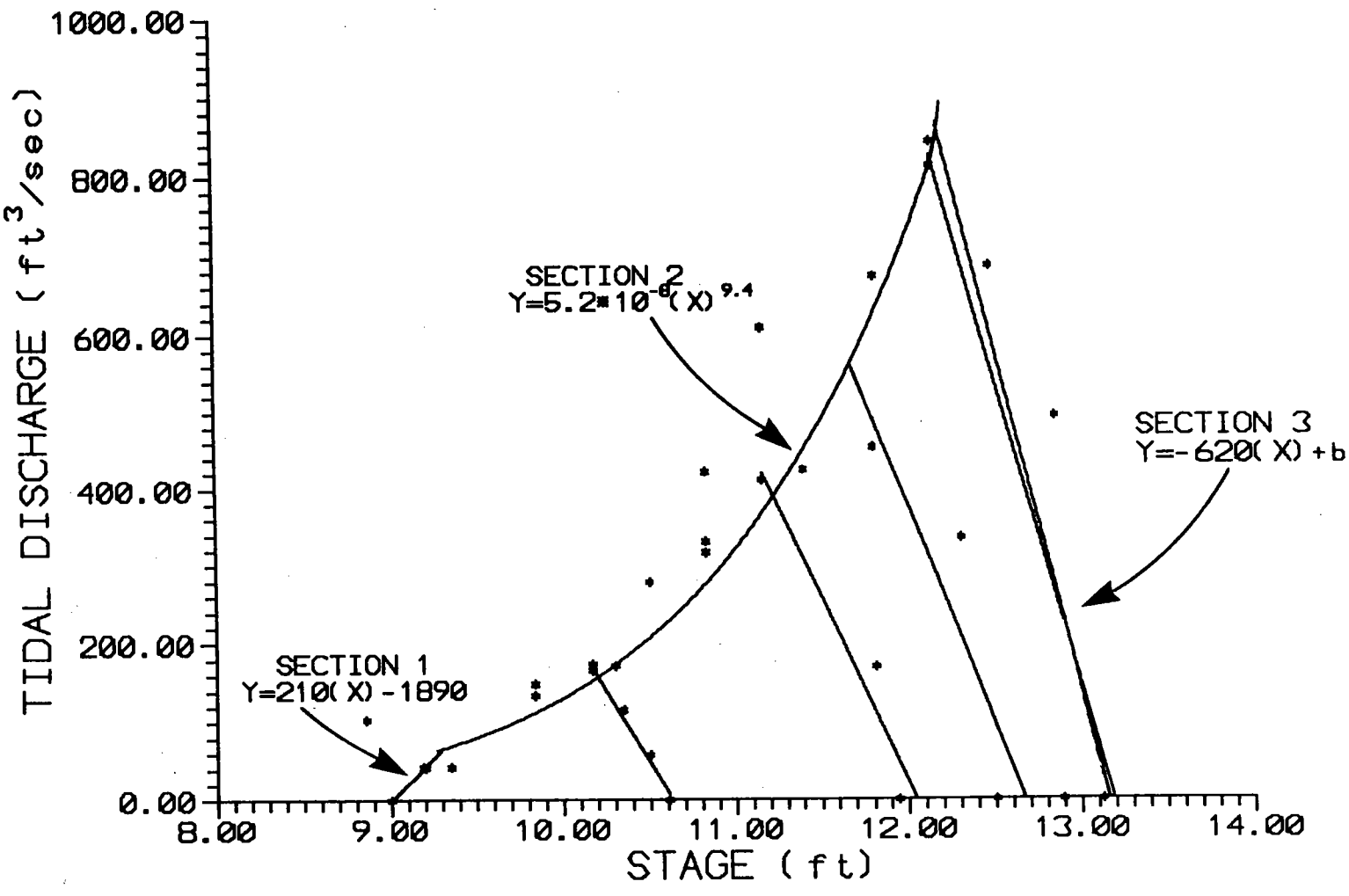

Figure 7A: Tidal discharge prediction function for channel 2, Tivoli North Bay, Hudson River National Research Reserve.

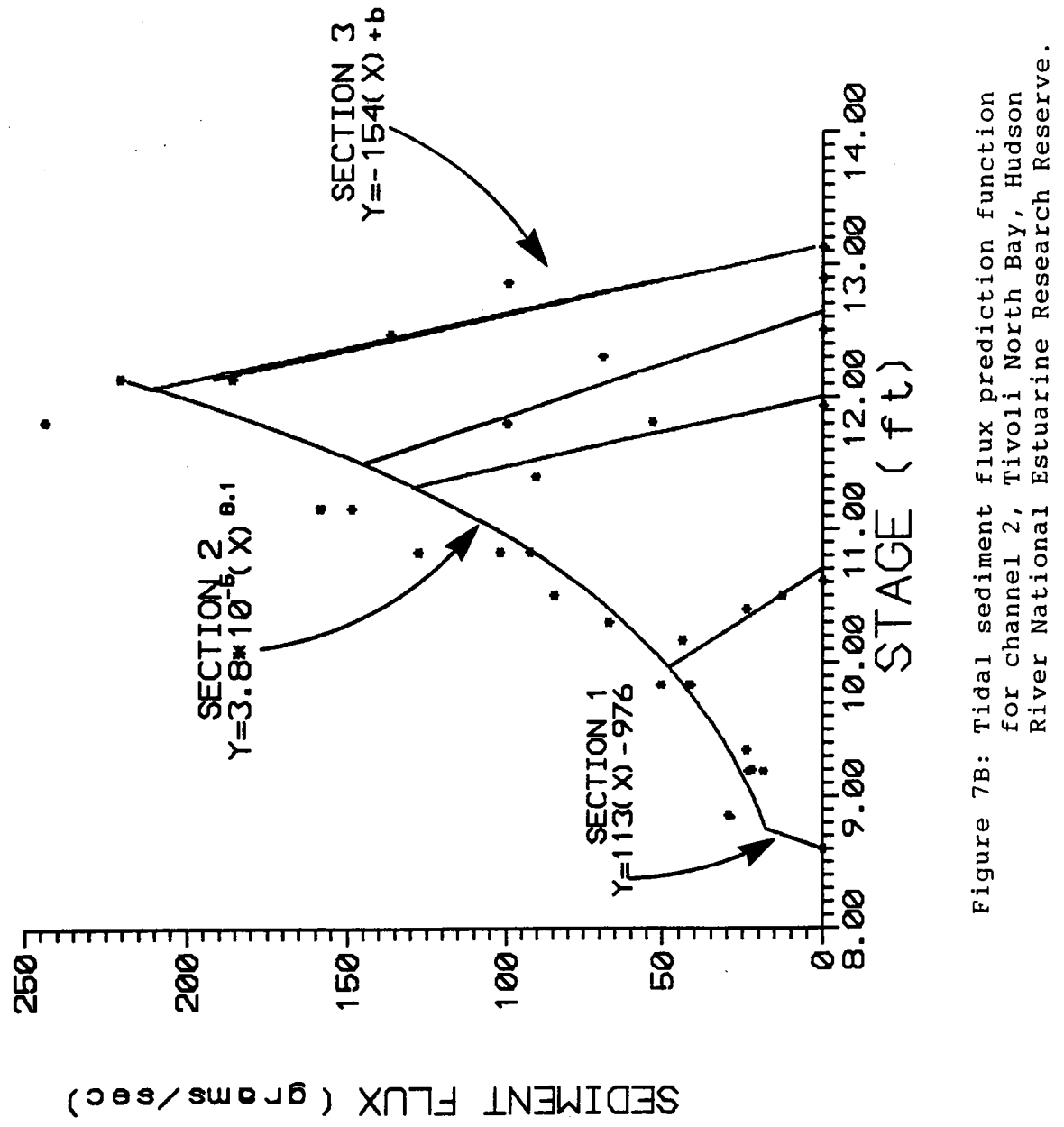

Figure 7B: Tidal sediment flux prediction function for channel 2, Tivoli North Bay, Hudson River National Estuarine Research Reserve.

Each prediction function has three sections. Using Figure 6A as an example, section 1 is a linear equation, of the form Y=mX+b, showing the relationship between discharge (or sediment flux) versus channel stage. Section 1 ranges from the low tide point to where it intersects with section 2. This line indicates the rapid rise in discharge over a short period of time, which is characteristic of tidal flows at the turn of a tide. Section 2 is an exponential equation, of the form $Y=aX^b$, that reflects the relationship between discharge or sediment flux versus channel stage. Section 2 ranges between the point of intersection with section 1 and the channel flow depth at which peak discharge occurs. This section is similar in form to a plot of discharge versus stage for any open channel (Linsley et al., 1975). Section 3 is again a linear equation, of the form Y=mX+b, showing the relationship between discharge (or sediment flux) versus channel stage for the interval between peak discharge and high tide. Section 3 has a unique position along the X-axis for each day of the lunar cycle. These prediction functions show a small degree of variation in slope for section 3. We use an average of these slopes to compute a specific section 3 equation for each prediction function. The validity of this approach will be tested with additional data collection during the on-going water balance study (Barten et al., in prep.).

DISCUSSION

The four prediction functions illustrated in Figures 6A, 6B, 7A, and 7B can be used to estimate instantaneous discharge and sediment flux values for any day of the lunar cycle. Plots of discharge and sediment flux versus time can be constructed from the series of instantaneous values. These data can be used to calculate the total flow volume and mass of transported sediment for a complete tidal cycle.

The utility of the discharge and sediment flux prediction functions is apparent when measuring environmental parameters directly correlated to tidal flow and sediment flux, such as nutrient and contaminant concentration. For example, it is necessary to pair pollutant concentration samples with discharge values in order to develop a mass balance. In most cases it is difficult to carry out field work required for pollutant or nutrient monitoring while simultaneously measuring the corresponding discharge.

Each of our four prediction functions are composed of three sections. Sections 1 and 2 have constant positions, while section 3 shifts along the x-axis throughout the lunar cycle. To solve these functions for instantaneous discharge and sediment flux the intersection points and x-intercepts must be determined for the particular tide levels. Figure 8 illustrates the four points defining two different tidal flows. Points C and D are the only two points that vary significantly during the lunar cycle. Points C' and D'

indicate this variability by showing a second tidal flow rating plot.

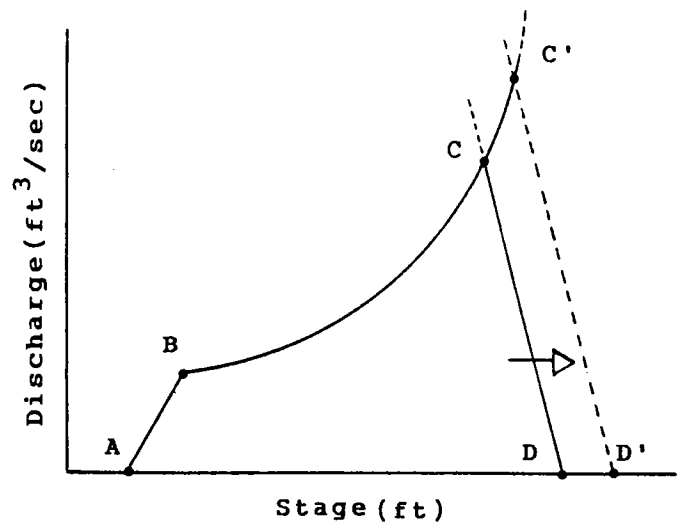

Figure 8: Generalized discharge prediction function showing two tidal flow events.

Point A is the low tide channel stage; it is nearly constant for channel 1 at 9.2 feet with a standard deviation of 0.19 feet. Channel 2 also has a nearly constant low tide channel stage of 8.9 feet with a standard deviation of 0.39 feet. Point B is determined by solving for the intersection point between sections 1 and 2. Point C is the channel stage where peak discharge occurs. This point is determined by solving for the intersection between sections 2 and 3. Point D is the high tide channel stage, which is obtained directly for each tidal flow by field measurement or water level recorder.

The three equations for sections 1, 2, and 3 shown on the four prediction functions are used to calculate a series of instantaneous discharge or sediment flux values ranging between low and high tide. The computational intervals and

form for each section of the prediction functions are listed below,

Section 1: $Y=mX+b$ ..... $A \leq X \leq B$

Section 2: $Y=aX^n$ ..... $B \leq X \leq C$

Section 3: $Y=mX+b$ ..... $C \leq X \leq D$

where:

Y = discharge (ft^3/sec) or sediment flux (g/sec)

X = stage

a = coefficient

b = intercept

m = slope

n = exponent

A = x-intercept at low tide

B = intersection of sections 1 and 2

C = intersection of sections 2 and 3

D = x-intercept at high tide

The complete example in Appendix A of this paper illustrates the process for calculating instantaneous discharge values for a particular tidal flow. This example demonstrates the small amount of field data needed to estimate total tidal flow volume or mass of transported sediment with these prediction functions for Tivoli North Bay.

The tidal discharge and sediment flux prediction functions shown in Figures 6A, 6B, 7A, and 7B exhibit two components that require additional explanation. First, are

the sharp intersection points where sections of the prediction function meet. Future research will focus on measurements in these regions to better approximate the equations representing each of the three sections. Once these regions are better defined it may be possible to fit a continuous function, a third order polynomial, for each tidal cycle.

The second component of the prediction functions requiring further explanation is the non-constant variance of the data points used to determine the power curves (sections 2). These data show less variability of points closer to the low tide region than farther up the curve in the region of peak discharge. This trend could be primarily attributed to greater sampling error near peak discharge. However, while it is possible that a larger sampling error was generated when measuring flow velocities near peak discharge (because of the difficulty of making measurements from a boat in a fast moving current), it is unlikely that this error would singularly account for the range in discharge values for a single stage indicated by these data. This variation also may be produced by the occurrence of multiple discharge values at a given stage in the vicinity of peak discharge. Again, this uncertainty could be reduced by replication and subsequent refinement of the prediction functions.

The occurrence of multiple discharge values at a single channel stage can in part explain the appearance of the

greater variability of data points in the regions of peak discharge for the power equations of the four prediction functions. Figures 5A and 5B show that the total flow volume and sediment mass exchanged through channels 1 and 2 can vary by a factor of 2 in the nearly constant six hour flow period. Two factors appear to enable the channel to accommodate these larger tidal flows, which also helps to explain the occurrence of multiple discharge values at a single channel stage. One is the simple rise in the overall water elevation as indicated by the range in high tide marks. The second is an increase in average flow velocity generated in response to a larger water surface gradient between the tidal source, the Hudson River, and Tivoli North Bay. Average flow velocities for three tidal cycles that demonstrate this trend are listed in Table 4.

Table 4: Average flow velocity for three tidal flows at channel 1, North Tivoli Bay.

Total Tidal Flow Volume (ft^3)	Average Flow Velocity (ft/sec)
4,400,000	0.35
6,700,000	0.52
10,000,000	0.81

It follows that increases in average flow velocity result in greater discharge values. The occurrence of multiple

discharge values at a single stage, shown on the prediction functions, is most apparent in the region of peak discharge. This overlap exists because the peak discharge for one tidal flow often corresponds to a discharge value prior to or after peak discharge for a second tidal flow. In summary, two factors are proposed to explain the greater degree of variability in discharge estimates at the upper segments of the power curves. They are (1) a larger sampling error generated by the difficulty of measuring flow velocity in strong currents and, (2) an increase in average flow velocity for certain tidal flows of the lunar cycle.

Discharge and sediment prediction functions similar to those developed during this study were not found in the relevant literature. As awareness increases that estuarine systems like the HRNERR are hydrologically and ecologically important, a greater emphasis will be directed towards quantifying water flow and sediment transport because of their importance as principal transport mechanisms. The field methods and mathematical analyses that were developed and applied during this study can be readily adapted to other estuarine systems.

ACKNOWLEDGEMENTS

I thank the Hudson River Foundation and the New York State Department of Environmental Conservation, Hudson River National Estuarine Research Reserve for funding this project. In particular, I am grateful to John Waldman and Betsy Blair for their assistance and support; Tom Marchesi and Larry Warshaw for their assistance in the field.

References

Anderson, H.W., M.D. Hoover., and K.H. Reinhart. 1976. Forests and water: effects of forest management on floods, sedimentation, and water supply. USDA Forest Service General Technical Report PSW-18/1976.

Butler, S.S. 1957. Engineering Hydrology. Prentice Hall, New Jersey.

Dunne, T. and L.B. Leopold. 1978. Water in Environmental Planning. W.H. Freeman Co., New York.

Dyer, K.R. 1979. Estuarine Hydrography and Sedimentation. Cambridge University Press, Cambridge.

Goldhammer, A. and S. Findlay. 1988. Estimation of Suspended Material Flux Between a Trapa natans stand and the Hudson River Estuary. Pages VIII-46 in J.R. Waldman and E.A. Blair, editors. Final reports of the Tibor T. Polgar Fellowship Program, 1988. Hudson River Foundation, New York, New York

Guy, H.P. 1970. Fluvial Sediment Concepts. USGS, Techniques of Water-Resources Investigations of the United States Geological Survey, Book 3: Applications of Hydraulics, Chapter C1.

Guy, H.P., 1969. Laboratory Theory and Methods for Sediment Analysis. USGS. Techniques of Water-Resources Investigations of the United States Geological Survey, Book 5, Chapter C1.

Guy, H.P. and V.W. Norman. 1970. Field Methods for Measurements of Fluvial Sediment. USGS. Techniques of Water-Resources Investigations of the United States Geological Survey, Book 3, Chapter C2.

King, H.W. and E.F. Brater. 1963. Handbook of Hydraulics. Mcgraw-Hill, New York. Fifth Edition.

Lickus, M.R. and P.K. Barten. 1990. Hydrology of Freshwater Tidal Marsh in the Hudson Estuary. (In Press).

Laronne, J.B. and M.P. Mosley. 1982. Erosion and Sediment Yield. Hutchinson Ross Publishing Company, Pennsylvania.

Linsley, Jr. R.K., M.A. Kohler, and J.H. Paulhus. 1958. Hydrology for Engineers. New York. Second Edition.

Nuttle, W.K. 1988. Extent of lateral movement in the sediments of a New England salt marsh. Water Resources Research 24(12):2077-2085.